Supporting Information

Sodium citrate as cathode pre-sodiation additive for sodium ion batteries

Rui Zhang‡[a,b], Zheng Tang‡[a], Dan Sun[a]*, Ruiyi Li[a], Wenhao Yang[a], Siyu Zhou[a], Zhiyong Xie[b*], Yougen Tang[a] and Haiyan Wang[a*]

[a] *Hunan Provincial Key Laboratory of Chemical Power Sources, College of Chemistry and Chemical Engineering, Central South University, Changsha, 410083, P.R. China*

[b] *Powder Metallurgy Institute, Central South University, Changsha, 410083, P.R. China*

*E-mail address: wanghy419@126.com; sundan4330@csu.edu.cn; xzy507@csu.edu.cn
‡ Rui Zhang and Zheng Tang contributed equally to this work.

Experimental Section

1.1 Synthesis of cathode materials

The synthesis of $Na_3V_2(PO_4)_2F_3$/rGO (NVPOF/rGO) cathode material referred to the previous literature.[S1] All chemical reagents used in this work are analytical grade. V_2O_5 (364 mg) and $H_2C_2O_4 \cdot 2H_2O$ (648 mg) were dissolved in 30 mL deionized water under continuous stirring at 80 °C for 30 min. Subsequently, $NH_4H_2PO_4$ (460 mg) and NaF (252 mg) were added into the blue solution. After another 30 min, 750 mg polyvinyl pyrrolidone (K30) was added to the above solution under stirring until it dissolved completely. Then, 22.5 mL commercial graphene oxide (GO) suspension (≈2 mg mL^{-1}, Tanfeng Tech) was poured into the prepared solution with stirring for 60 min. The black mixture was transferred to a 100 mL Teflon-lined stainless steel autoclave and kept in an electrical oven at 170 °C for 9 h. The black precipitate was obtained via centrifugal separation and washed three times with deionized water. The precursor was dried by a freeze dryer and further annealed in Ar atmosphere at 650 °C for 2 h to get the final product.

1.2 Preparation of electrodes

1.2.1 Preparation of sodium citrate electrode

SC electrode was prepared by mixing sodium citrate (SC), Ketjenblack (KB) and polyvinylidene fluoride (PVDF) in N-methylpyrrolidone (NMP) according to the mass

ratio of 70:20:10 to obtain the uniform slurry. And the slurry was spread onto the aluminum foil and then dried at 100 ^{o}C for 12 h in a vacuum oven. The electrodes were finally punched into disks with 12 mm in diameter. The mass loading of SC electrode was about 2 mg cm^{-2}.

1.2.2 Preparation of cathode electrode

NVPOF/rGO electrode was prepared by mixing NVPOF/rGO, KB and PVDF in NMP according to the mass ratio of 80:10:10 to obtain the uniform slurry. And the slurry was spread onto the aluminum foil and then dried at 100 ^{o}C for 12 h in a vacuum oven. NVPOF/rGO with 10 wt% SC additive (NVPOF/rGO-10) was prepared as the similar process except that the extra 10 wt% SC based on the total mass of NVPOF/rGO, KB and PVDF was added in the mixing stage. Similarly, NVPOF/rGO with 20 wt% SC additive (NVPOF/rGO-20) was also prepared. The electrodes were finally punched into disks with 12 mm in diameter. The mass loading of cathode electrode for half cell was ~1.8 mg cm^{-2}, and the mass loading of cathode electrode for full cell was about 4.6 mg cm^{-2}.

1.2.3 Preparation of anode electrode

The anode electrode was prepared by mixing commercial hard carbon (CHC), KB and PVDF in NMP according to the mass ratio of 80:10:10 to obtain the uniform slurry. And the slurry was spread onto the copper foil and then dried at 100 ^{o}C for 12 h in a vacuum oven, which was noted as CHC electrode. The electrodes were finally punched into disks with 12 mm in diameter. The mass loading of CHC electrode was about 1 mg cm^{-2}.

1.3 Material characterization

The crystal structures of samples were characterized by X-ray diffraction (XRD, Rigaku, Cu Kα radiation). X-ray photoelectron spectroscopy (XPS, ESCALAB250Xi) was conducted to detect the surface valence state of samples. Field-emission scanning electron microscopy (FE-SEM, Nova NanoSEM 230) characterize the morphological structures of electrode. Nuclear magnetic resonance (NMR, BRUKER AVANCE 400) and ttenuated total reflection fourier transform infrared spectroscopy (ATR-FTIR, Bruker Vertex 70) were applied to investigate the structure of organics. Gas

chromatography (GC) was performed to determine the gas components.

1.4 Electrochemical measurements

Electrochemical performances were evaluated with CR2025 coin cells. The cells were assembled in an argon-filled glovebox using 1 M $NaClO_4$ dissolved in propylene carbonate (PC) with 5 vol% fluoroethylene carbonate (FEC) as the electrolytes and glass fiber as the separators. For the half cells, the anodes were home-made sodium foils, while those of the full cells were CHC electrodes. Galvanostatic charge/discharge tests were conducted with Neware battery system. Before characterizing cycled electrodes, these electrodes would be washed with dimethyl carbonate (DMC) to remove the electrolyte from the electrode surface and dried in vacuum at room temperature.

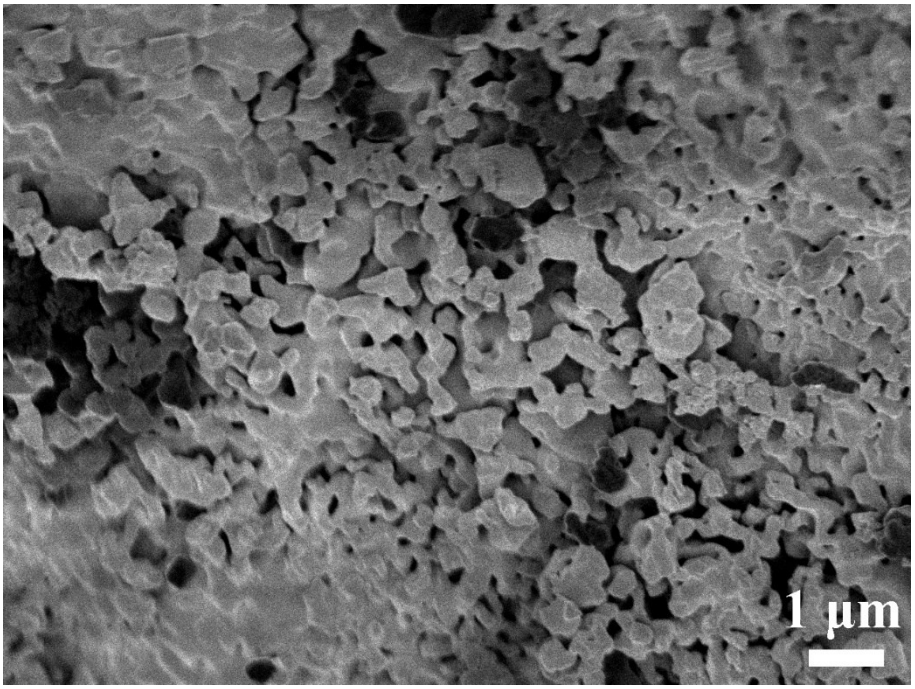

Fig S1. SEM image of commercial SC reagent.

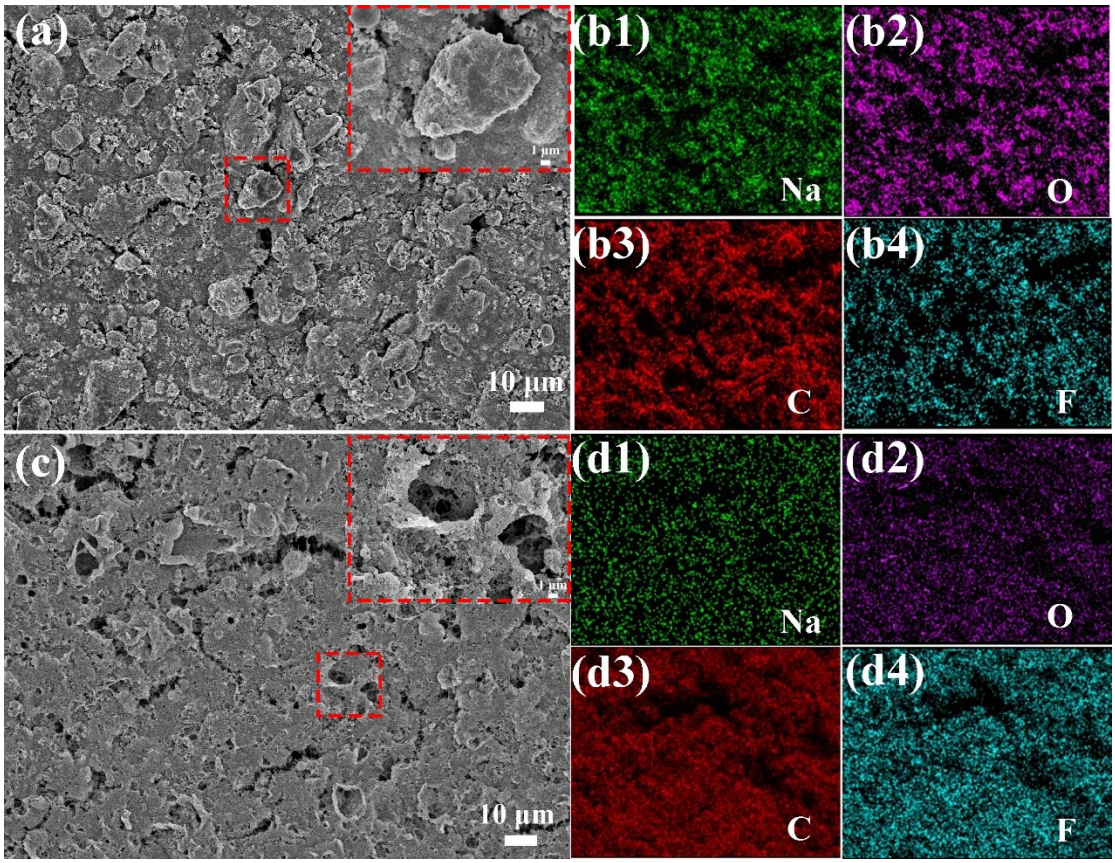

Fig S2. SEM images of fresh SC electrode (a) and fully charged SC electrode (c) (Insets are the enlarged pictures of local areas). EDX mapping images (Na, O, C, F) of SC electrode (b1-b4) and fully charged SC electrode (d1-d4)

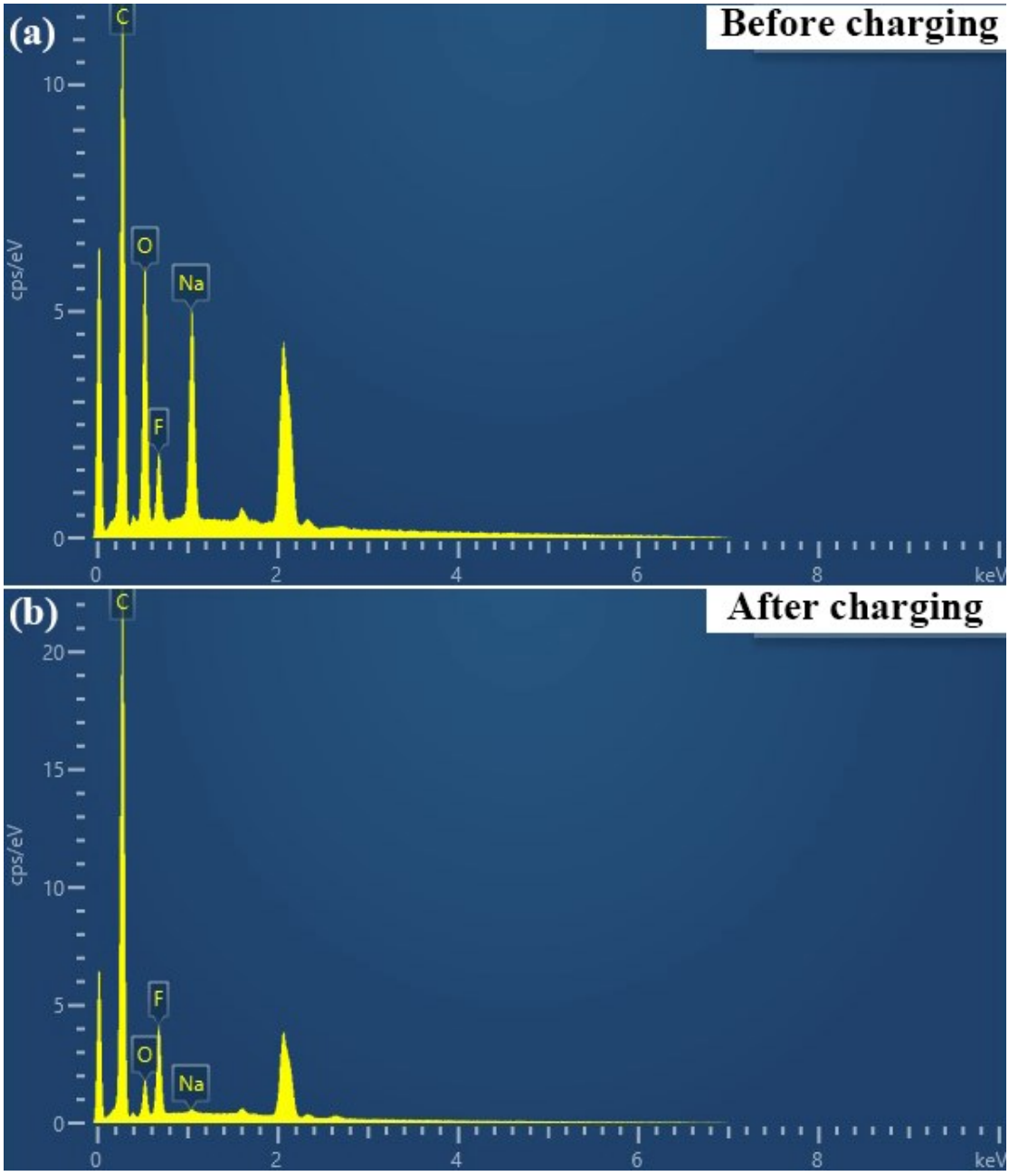

Fig S3. EDX spectra of SC electrode before charging (a) and after charging (b).

Table S1. The element contents of Na, O, C and F in the SC electrode before and after cycling

Element	Before charging /wt%	After charging /wt%
Na	16.8	0.4
O	25.9	8.3
C	49.1	73.0
F	8.2	18.3

Table S2. The proportion of C 1s groups in the SC electrode before and after charging

Sample	C=C/C-C	C-O	C=O	COONa/COOH	CFx
Fresh SC electrode	49.98%	11.03%	17.83%	9.95%	11.21%
The charged SC electrode	37.78%	14.77%	27.58%	5.07%	14.80%

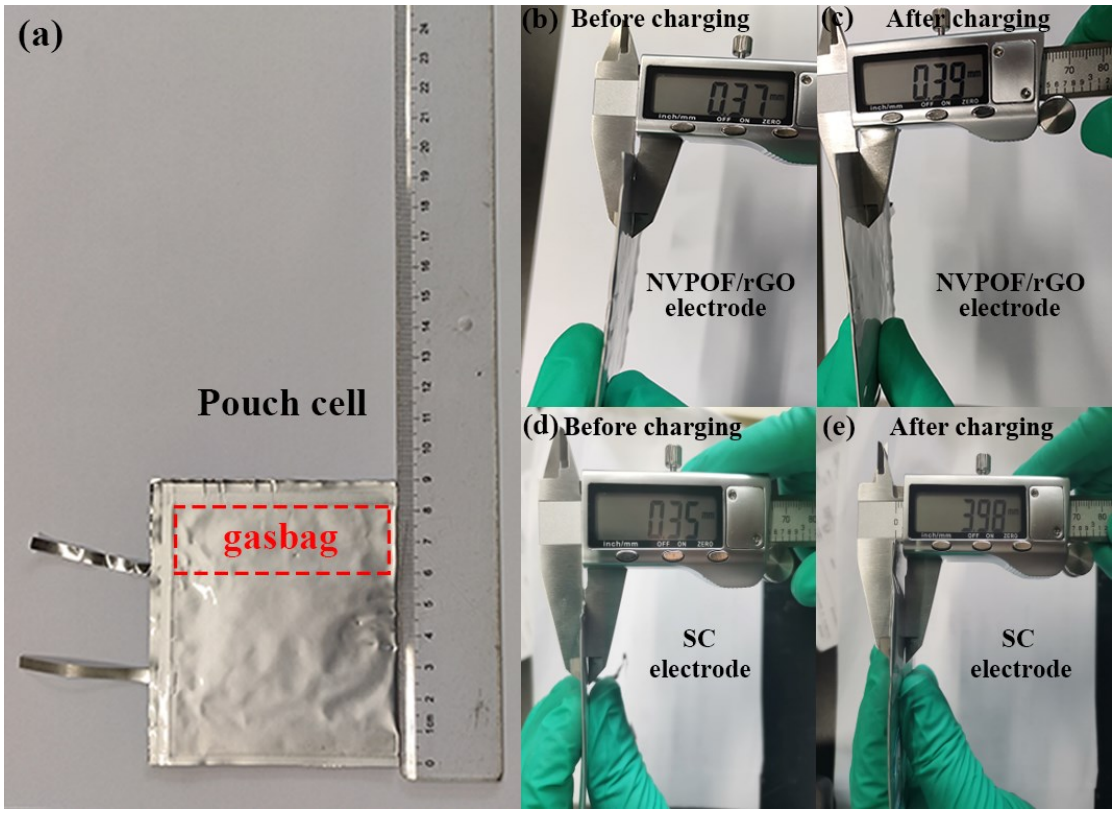

Fig S4. (a) The optical photograph of assembled pouch cell with the Na foil as the reference electrode and counter electrode. The side view of NVPOF/rGO pouch cell before (c) and after charging (d). The side view of SC pouch cell before (c) and after charging (d).

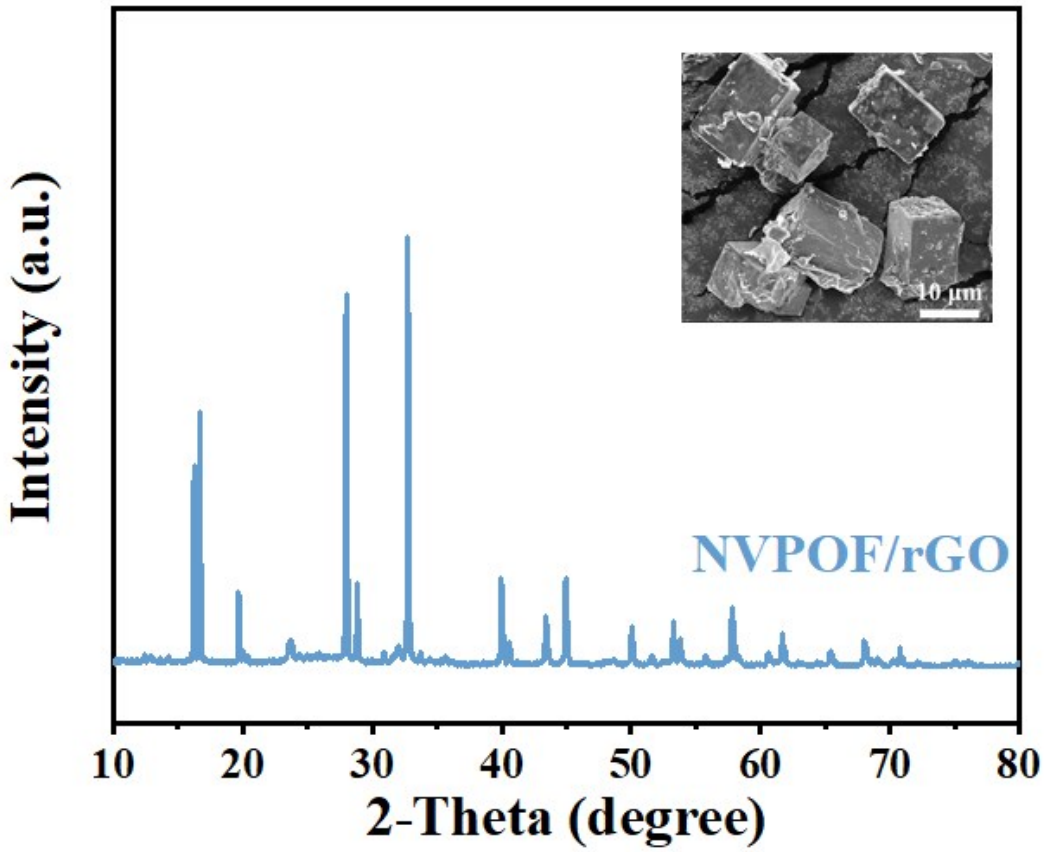

Fig S5. XRD pattern of the synthesized NVPOF/rGO (inset is the SEM image).

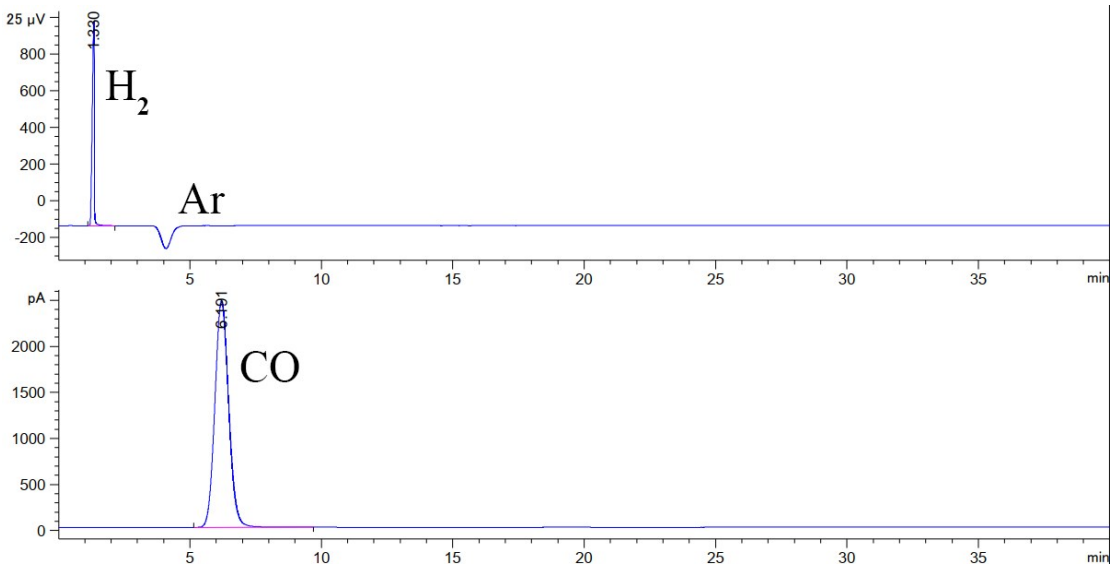

Fig S6. Gas chromatography of the gas collected from the gasbag of charged SC pouch cell.

The gas chromatographic result reveals the existence of CO and H_2 clearly, and no O_2 is found. Moreover, in Fig 1c, the initial charge capacity of SC electrode is only 330 mAh g-1, which is close to its theoretical value. If this process involves the formation and electrolysis of H_2O molecular or other unknown side reactions, SC electrode will lose more electrons and the corresponding charge capacity should be far more than 330 mAh g-1. Hence, the decomposition mechanism of SC is significantly different from the reported cathode additives, EDTA-4Na and DTPA-5Na,[S2, S3] which might be ascribed to different chemical environment at which sodiated carboxyl groups locate. For EDTA-4Na/ DTPA-5Na, the CH2-COONa groups are liked with N atom to form N-CH2-COONa,1, 2 while the CH2-COONa groups in SC are linked with C atom to form C-CH2-COONa.

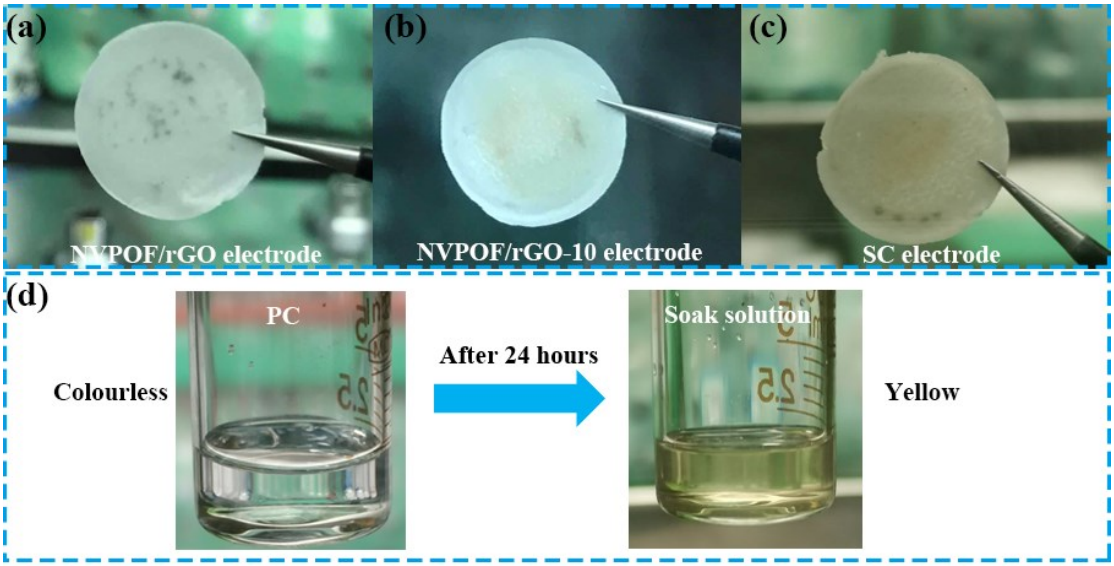

Fig S7. Optical photographs for the separators of cycled NVPOF/rGO electrode (a), NVPOF/rGO-10 electrode (b) and SC electrode (c). (d) The soak solution with the separator of cycled SC electrode immersed in PC solvent for 24 hours.

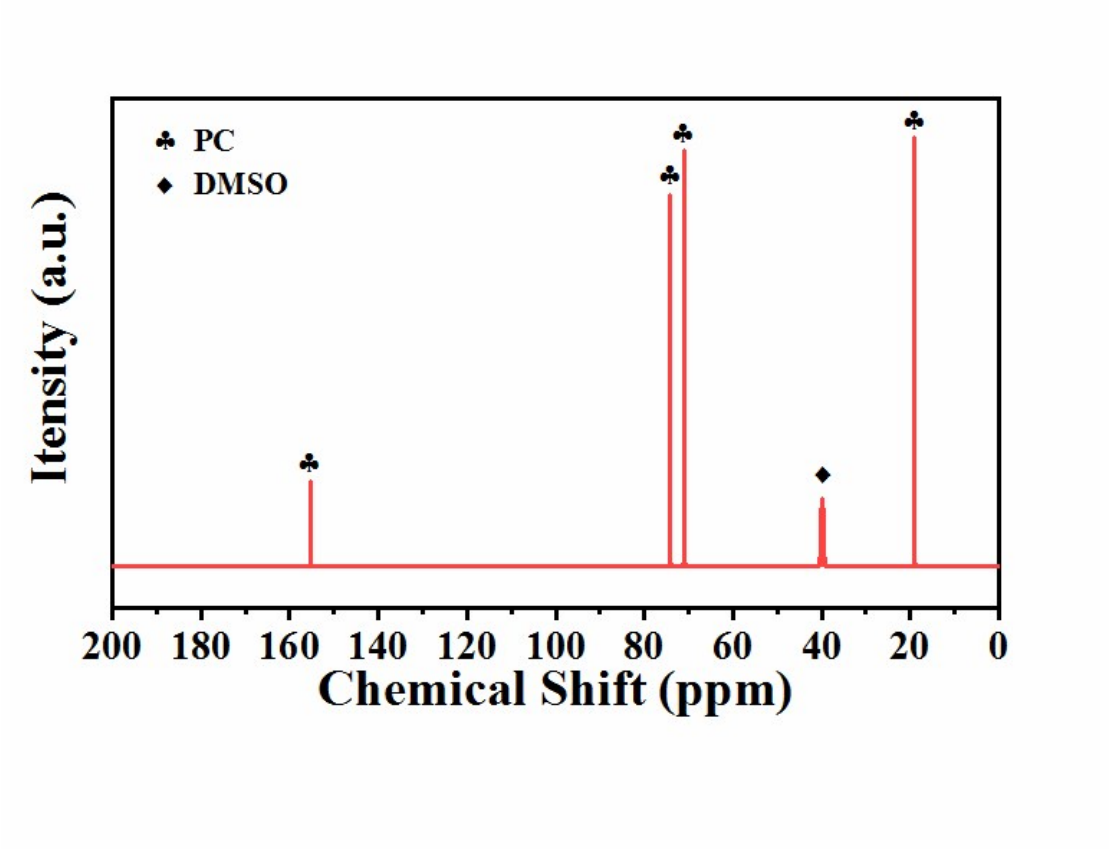

Fig S8. 13C NMR spectra of the soak solution obtained from Fig S6d.

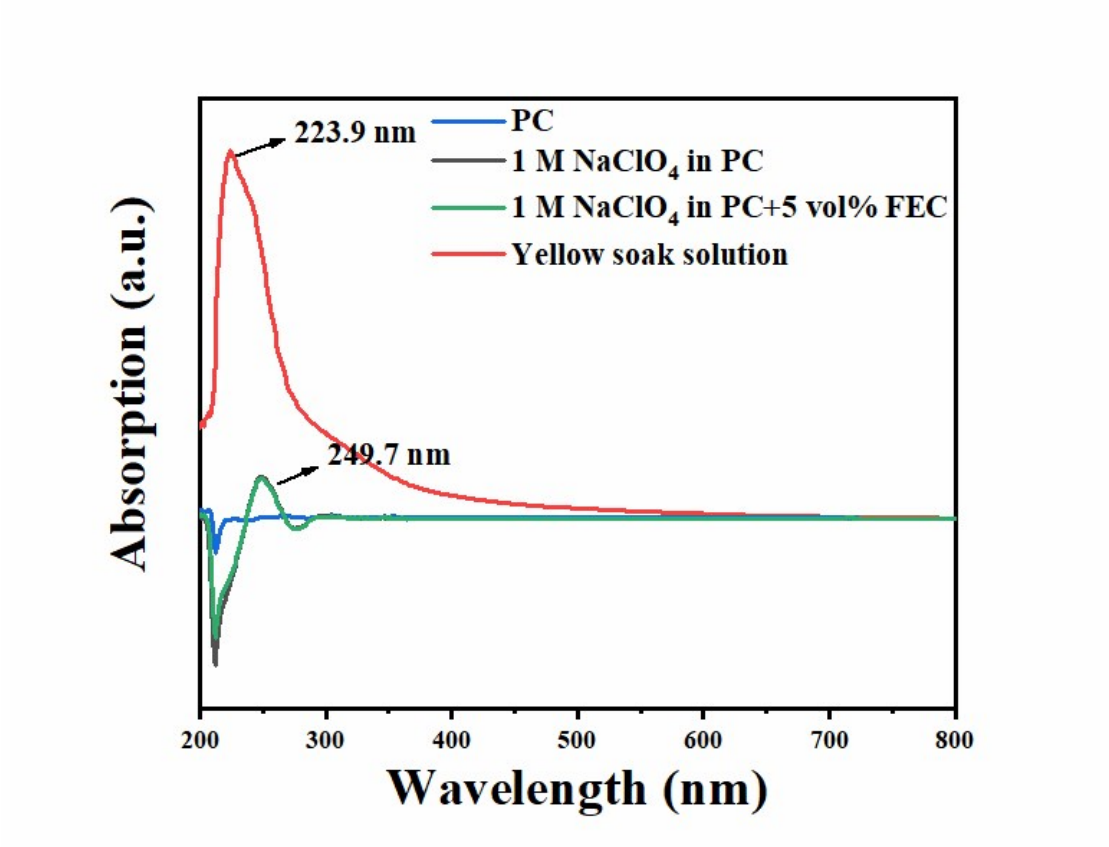

Fig S9. UV-vis spectra of PC solvent, yellow soak solution and different electrolytes.

In Fig S9, PC solvent and other PC-based electrolyte show no absorption at visible region (390-780 nm). In contrast, the PC soaking solution has weak adsorption of visible light, indicating the exist of large conjugated structure in the yellow residue. Noting that a strong adsorption peak at 223.9 nm is also observed in the UV-vis spectrum of yellow soaking solution, which should be ascribed to $NaClO_4$ salt dissolved in the yellow soak solution and other unknown matters. It is speculated that these unknown matters might originate from the further decomposition of these yellow residues.

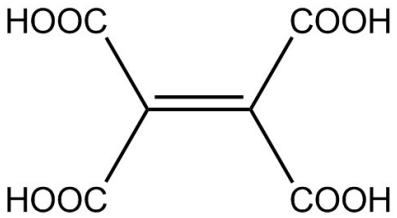

Fig S10. Chemical structural formula of 1,1,2,2-ethenetetracarboxylicacid.

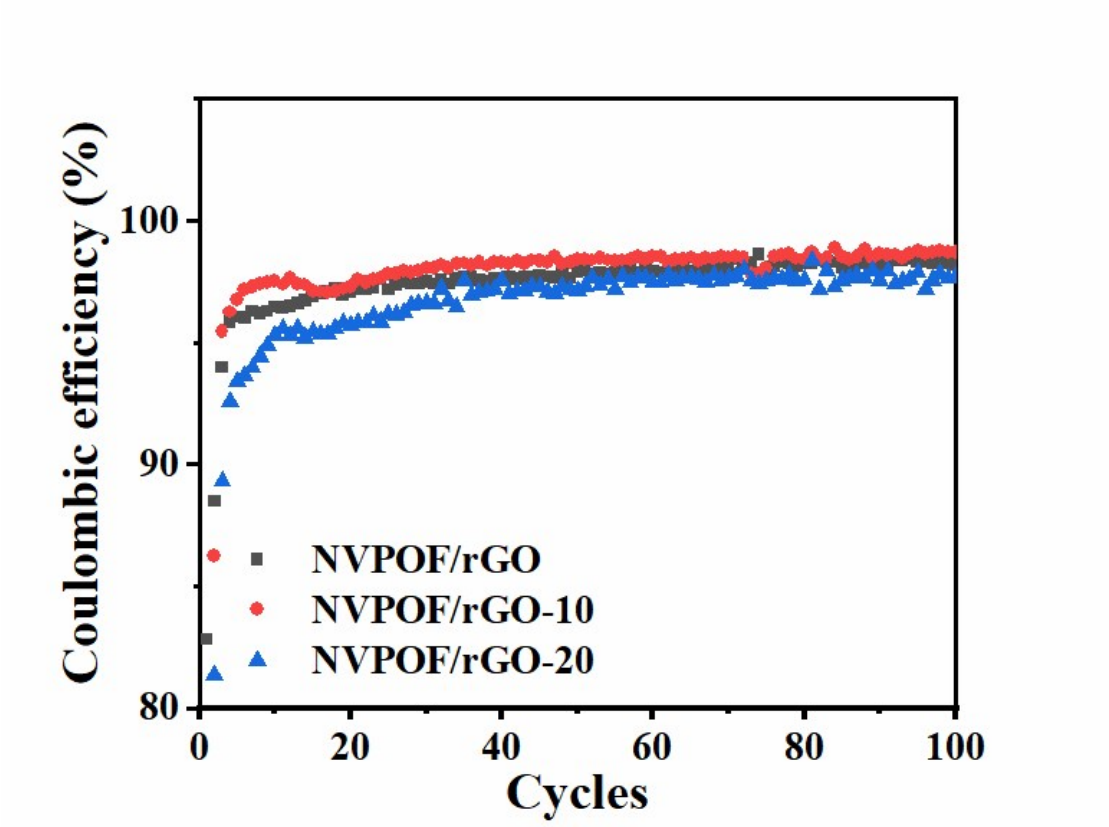

Fig S11. Comparison of Coulombic efficiencies of half-cells with different amounts of SC additive (0 wt%, 10 wt% and 20 wt%) cycled at 50 mA g^{-1}.

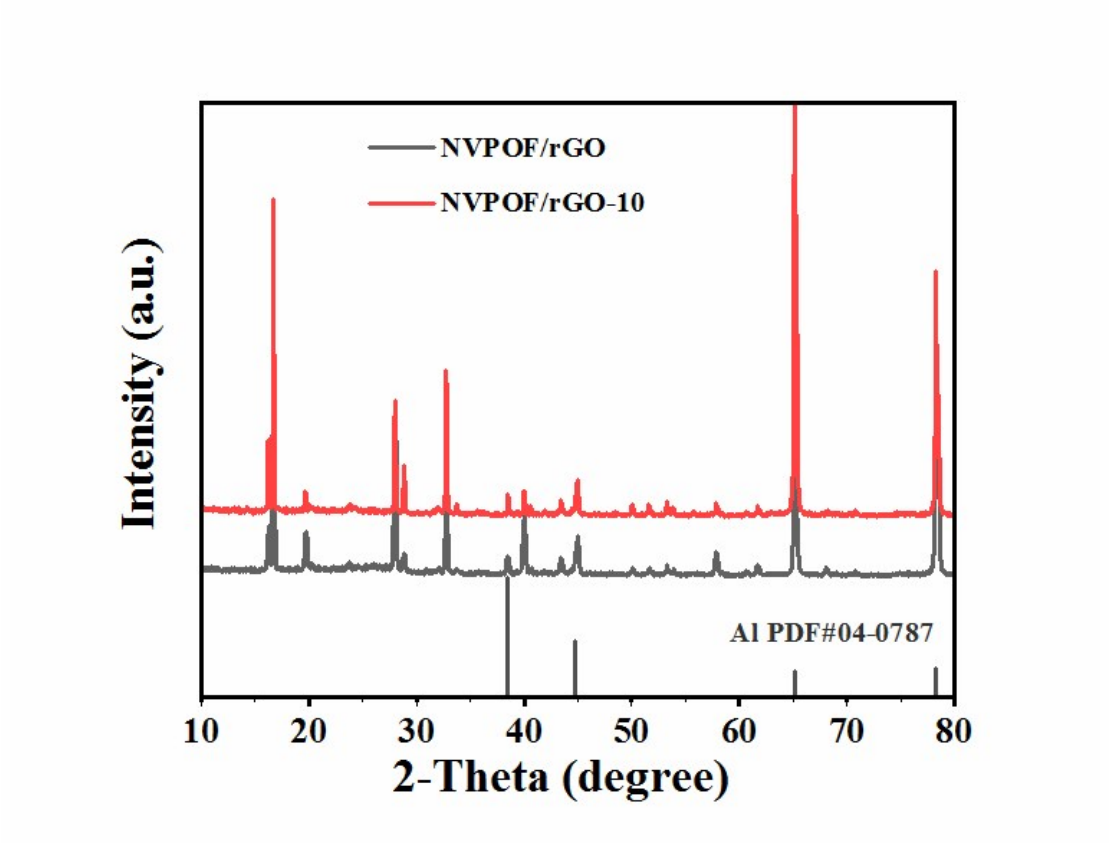

Fig S12. XRD patterns of NVPOF/rGO and NVPOF/rGO-10 electrodes after cycles.

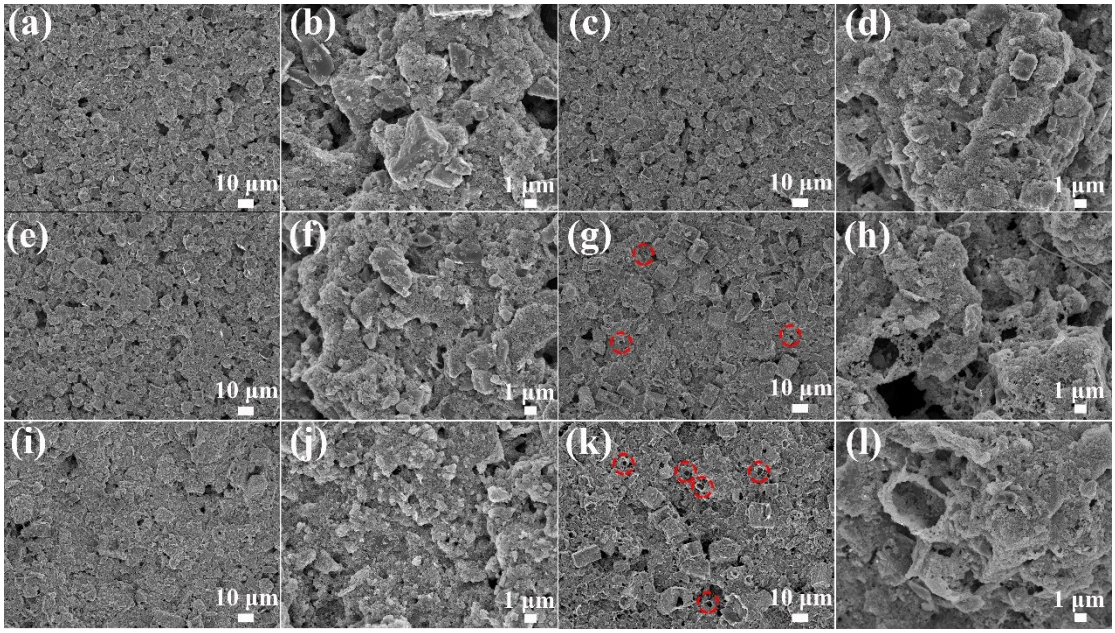

Fig S13. SEM images of different electrodes before and after cycles. Surface images of NVPOF/rGO electrode before (a, b) and after (c, d) cycles. Surface images of NVPOF/rGO-10 electrode before (e, f) and after (g, h) cycles. Surface images of NVPOF/rGO-20 electrode before (i, j) and after (k, l) cycles.

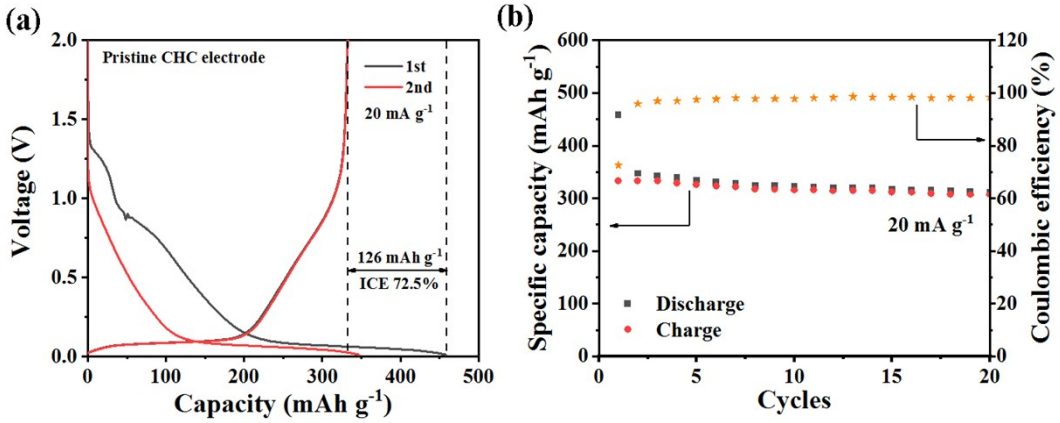

Fig S14. (a) Galvanostatic charge/discharge curves of pristine CHC electrode. (b) Cycling performance and Coulombic efficiency of CHC electrode.

Table S3. Comparison of physical and electrochemical properties of reported sodium compensation additives

Additive	Decomposition voltage (V)	Theoretical capacity (mAh g^{-1})	Actual capacity (mAh g^{-1})	Utilization (%)	Freiendliness	Ref
Na_3P	0.5	804	~600	74.6	Toxicity, flammability	S4
$NaCrO_2$	3.8	250.5	235	93.8	Toxicity	S5
NaN_3	3.55	412	270	65.5	Toxicity, explosivity	S6
$Na_2C_4O_4$	3.6	339	230	67.8	Good	S7
$NaNO_2$	3.4	427	~350	81.9	Toxicity, explosivity, flammability	S8
EDTA-4Na	3.79	282	-	-	Good	S2
Na_2CO_3	4	505	90	17.8	Good	S9
$Na_2C_2O_4$	4.11	400	396.9	99.2	Good	S10
SC	4.0	312	302	96.8	Good	This work

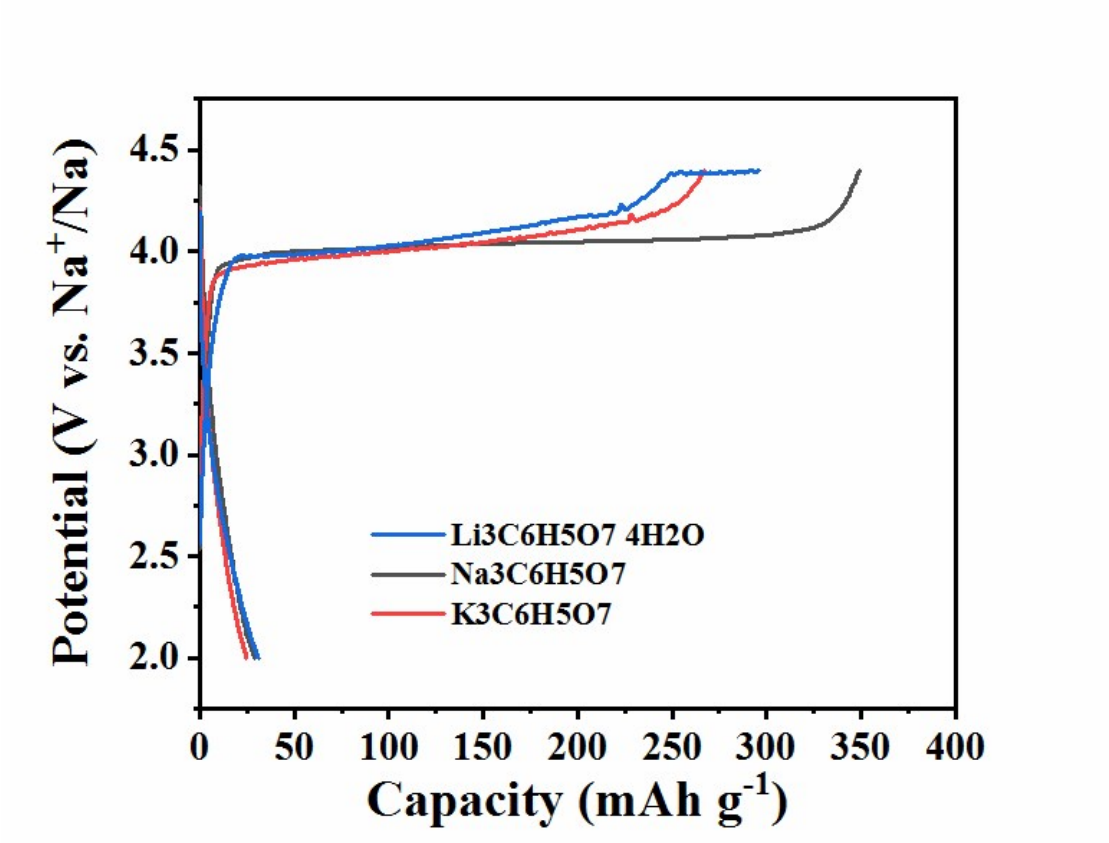

Fig S15. Galvanostatic charge/discharge curves of lithium citrate tetrahydrate, sodium citrate and potassium citrate electrodes at 20 mA g^{-1}.

Reference

[S1] Y. Cai, X. Cao, Z. Luo, G. Fang, F. Liu, J. Zhou, A. Pan and S. Liang, *Adv. Sci.*, 2018, **5**, 1800680.

[S2] J. H. Jo, J. U. Choi, Y. J. Park, J. Zhu, H. Yashiro and S. T. Myung, *ACS Appl Mater. Interfaces*, 2019, **11**, 5957-5965.

[S3] J. H. Jo, J. U. Choi, Y. J. Park, J. K. Ko, H. Yashiro and S.-T. Myung, *Energy Storage Mater.*, 2020, **32**, 281-289.

[S4] B. Zhang, R. Dugas, G. Rousse, P. Rozier, A. M. Abakumov and J. M. Tarascon, *Nat. Commun.*, 2016, **7**, 10308.

[S5] B. Shen, R. Zhan, C. Dai, Y. Li, L. Hu, Y. Niu, J. Jiang, Q. Wang and M. Xu, *J. Colloid Interface Sci.*, 2019, **553**, 524-529.

[S6] J. M. De Ilarduya, L. Otaegui, L. D. A. Miguel, Juan, M. Armand and G. Singh, *J. Power Sources*, 2017, **337**, 197-203.

[S7] D. Shanmukaraj, K. Kretschmer, T. Sahu, W. Bao, T. Rojo, G. Wang and M. Armand, *ChemSusChem*, 2018, **11**, 3286-3291.

[S8] C.-H. Jo, J. U. Choi, H. Yashiro and S.-T. Myung, *J. Mater. Chem. A*, 2019, **7**, 3903-3909.

[S9] M. Sathiya, J. Thomas, D. Batuk, V. Pimenta, R. Gopalan and J.-M. Tarascon, *Chem. Mater.*, 2017, **29**, 5948-5956.

[S10] Y. B. Niu, Y. J. Guo, Y. X. Yin, S. Y. Zhang, T. Wang, P. Wang, S. Xin and Y. G. Guo, *Adv. Mater.*, 2020, **32**, 2001419.